International Journal of Nanomedicine

Dovepress
open access to scientific and medical research

Open Access Full Text Article

ORIGINAL RESEARCH

In vitro and in vivo evaluation of SN-38 nanocrystals with different particle sizes

This article was published in the following Dove Press journal:
International Journal of Nanomedicine
1 August 2017
Number of times this article has been viewed

Min Chen[1,2]
Wanqing Li[3]
Xun Zhang[1]
Ye Dong[1]
Yabing Hua[1]
Hui Zhang[1]
Jing Gao[1]
Liang Zhao[2]
Ying Li[1]
Aiping Zheng[1]

[1]State Key Laboratory of Toxicology and Medical Countermeasures, Beijing Institute of Pharmacology and Toxicology, [2]School of Pharmacy, Jinzhou Medical University, Jinzhou, [3]School of Preclinical Medicine, Beijing University of Chinese Medicine, Beijing, People's Republic of China

Abstract: 7-Ethyl-10-hydroxycamptothecin (SN-38) is a potent broad-spectrum antitumor drug derived from irinotecan hydrochloride (CPT-11). Due to its poor solubility and instability of the active lactone ring, its clinical use is significantly limited. As one of the most promising formulations for poorly water-soluble drugs, nanocrystals have attracted increasing attention. In order to solve these problems and evaluate the antitumor effect of SN-38 in vitro and in vivo, two nanocrystals with markedly different particle sizes were prepared. Dynamic light scattering and transmission electron microscopy were used to investigate the two nanocrystals. The particle sizes of SN-38 nanocrystals A (SN-38/NCs-A) and SN-38 nanocrystals B (SN-38/NCs-B) were 229.5±1.99 and 799.2±14.44 nm, respectively. X-ray powder diffraction analysis showed that the crystalline state of SN-38 did not change in the size reduction process. An accelerated dissolution velocity of SN-38 was achieved by nanocrystals, and release rate of SN-38/NCs-A was significantly faster than that of SN-38/NCs-B. Cellular uptake, cellular cytotoxicity, pharmacokinetics, animal antitumor efficacy, and tissue distribution were subsequently examined. As a result, enhanced intracellular accumulation in HT1080 cells and cytotoxicity on different tumor cells were observed for SN-38/NCs-A compared to that for SN-38/NCs-B and solution. Besides, compared to the SN-38 solution, SN-38/NCs-A had a higher bioavailability after intravenous injection; while the bioavailability of SN-38/NCs-B was even lower than that of the SN-38 solution. SN-38/NCs-A exhibited a significant inhibition of tumor growth compared to SN-38 solution and SN-38/NCs-B in vivo. The antitumor effect of SN-38/NCs-B was stronger than SN-38 solution. The tissue distribution study in tumor-bearing mice showed that nanocrystals could markedly improve the drug accumulation in tumor tissue by the enhanced permeability and retention effect compared to SN-38 solution, and the amount of SN-38 in tumors of SN-38/NCs-A group was much more than that of SN-38/NCs-B group. In conclusion, nanocrystals dramatically enhanced the anticancer efficacy of SN-38 in vitro and in vivo, and the particle size had a significant influence on the dissolution behavior, pharmacokinetic properties, and tumor inhibition of nanocrystals.

Keywords: SN-38, nanocrystals, antitumor efficacy, cellular uptake, pharmacokinetics, tissue distribution

Introduction

7-Ethyl-10-hydroxycamptothecin (SN-38) is an analog of the natural anticancer alkaloid camptothecin (CPT). It is derived from irinotecan hydrochloride (CPT-11) via carboxylesterase (CE)-mediated de-esterification primarily in the liver.[1,2] SN-38 executes the therapeutic action through inhibiting the release of single-strand DNA by forming a ternary complex with topoisomerase I (TOPI) and DNA. This makes DNA replication fail and leads to cell death.[3,4] SN-38 is a prominent and broad spectrum antitumor agent, which is effective against numerous malignant tumors, including lung, colorectal, gastric, lymph, cervical, and ovarian cancers.[5]

Correspondence: Ying Li; Aiping Zheng
State Key Laboratory of Toxicology and Medical Countermeasures, Beijing Institute of Pharmacology and Toxicology, 27 Taiping Road, Beijing 100850, People's Republic of China
Tel +86 10 6687 4665; +86 10 6693 1694
Fax +86 10 6693 1694
Email liying.sky@126.com; apzheng@163.com

submit your manuscript | www.dovepress.com
Dovepress
http://dx.doi.org/10.2147/IJN.S133816

Compared to CPT-11, SN-38 is 100–1,000 times more potent in terms of antitumor effect.[6] The inhibition activity of SN-38 mainly depends on the presence of the lactone ring, which shows pH-dependent hydrolysis.[7,8] At pH ≤4.5, the active lactone ring is stable but converted to the inactive carboxylate form completely by hydrolysis at pH >9.0. At physiological pH (pH 7.4), the lactone ring is instable and hydrolyzes to form the inactive form, which significantly reduces the therapeutic effect.[8] In addition, SN-38 is extremely insoluble in water (11–38 μg/mL) and is poorly solubilized at 0.5% (w/w) in most physiologically compatible and pharmaceutically acceptable solvents.[5,9,10] As a result, SN-38 cannot be administered directly.

To exploit the full therapeutic potential of SN-38, a variety of drug delivery systems have been extensively investigated, including polymeric implants,[11] micelles,[12–14] liposomes,[15,16] polymer conjugates,[7,17] and nanoparticles.[9,18] Unfortunately, although these techniques enhanced the solubility of SN-38, there are also many inherent drawbacks, such as low encapsulation efficiency and low drug loading,[10,15] poor stability during conjugation process, and low final yield of polymer conjugates.[19] The use of solvents or encapsulating excipients not only limits drug loading but also may induce adverse side effects.

Nanocrystals have recently been applied to overcome the formulation issue of poorly soluble drugs and have attracted wide attention. They are a type of submicron colloidal dispersion system with a mean particle size between 10 and 1,000 nm.[20] The nanometer-scale particles have an enormous surface area, and nanocrystals can greatly increase the dissolution velocity and saturation solubility of insoluble drugs consequently improving their bioavailability.[21]

In the carrier-free colloidal drug delivery systems, there are only pure drug crystals and a minimum amount of stabilizers. These require no chemical solvents and, thus, offer high drug loading and a much improved drug tolerance without excipient toxicity.[22] Furthermore, nanocrystals can be administrated intravenously because of their small particle size and safe composition.[23] Now there are currently several commercially available brands of drug nanocrystals on the market involving oral and injectable formulations.[24] Apparently, nanocrystals have numerous advantages on delivering poorly soluble drugs. Herein, nanocrystal formulation was selected as a way to make the clinical use of SN-38 possible. It has been found that the particle size of nanosuspensions had a marked effect on the pharmacokinetic characteristics and the bioavailability of the nanosuspension dosage form.[25,26] Thus, to understand the behaviors of SN-38 nanocrystals in vitro and in vivo, two nanocrystals with markedly different particle sizes were prepared.

In this study, two SN-38 nanocrystals with different particle sizes were prepared via high-pressure homogenization (HPH). The characterization, pharmacokinetics, tissue distribution, and antitumor efficiency in vitro and in vivo were then studied. There were two main purposes of this study: 1) to develop a novel formulation of SN-38 with high antitumor efficiency by nanocrystal technology, and 2) to investigate the influence of particle size on the characterization and behavior of SN-38 nanocrystals in vitro and in vivo.

Materials and methods

Materials

SN-38 (purity >98%) was purchased from Dalian Meilun Biological Technology Co. Ltd. (Dalian, China). Soybean lecithin was obtained from Tywei Pharmaceutical (Shanghai, China). Poloxamer 188 was provided by BASF (Ludwigshafen, Germany). The 3-(4,5-dimethyl-thiazol-2-yl)-2,5-diphenyltetrazolium bromide (MTT) was received from Jingke Hondar Biological Technology Co. Ltd. (Beijing, China). Dimethylsulfoxide (DMSO) was purchased from Sinopharm Chemical Reagent Co. Ltd. (Shanghai, China). Fluorescent probes including 1,1′-dioctadecyl-3,3,3′,3′-tetramethylindodicarbocyanine, 4-chlorobenzenesulfonate salt (DID) and Propidium iodide (PI) and hematoxylin–eosin (HE) staining reagent were purchased from KeyGEN Biotech Co. Ltd. (Nanjing, China). Methanol and acetonitrile (high-performance liquid chromatography grade) were obtained from Thermo Fisher Scientific (Waltham, MA, USA). Human breast adenocarcinoma cells (MCF-7 cells), human fibrosarcoma cells (HT1080 cells), and human hepatoma cells (HepG2 cells) were obtained from the Cell Resource Centre of IBMS (Beijing, China). All other chemicals and reagents used were analytical grade.

Male Sprague Dawley rats weighing 180–220 g were obtained from the Laboratory Animal Center of Academy of Military Medical Sciences (Beijing, China). Female Nu/nu nude mice weighing 18–22 g were purchased from Vital River Laboratories (Beijing, China). All of the animal experiments in our study complied with the National Institutes of Health guide for the care and use of laboratory animals and were approved by the Beijing Institute of Pharmacology and Toxicology.

Preparation of SN-38 nanocrystals

SN-38 nanocrystals were prepared by HPH technology. In brief, SN-38 coarse powder (1%, w/v) was dispersed in an aqueous surfactant solution, containing 0.5% Poloxamer 188 (w/v) and 0.2% soybean lecithin under magnetic stirring. Then, the mixture was premilled by a scattered

emulsification homogenizer-C25 (HENC, Shanghai, China) at 19,000 rpm for 1 min. The suspensions were further processed via HPH by a nano homogenizer machine (ATS Engineering Inc., Shanghai, China). In order to prepare two nanocrystalline suspensions with different particle sizes, different procedures were applied. For SN-38 nanocrystals B (SN-38/NCs-B), five homogenization cycles at 200 bars were conducted first, as premilling step, and then, 30 homogenization cycles at 400 bars were run to obtain the nanocrystalline suspensions. For SN-38 nanocrystals A (SN-38/NCs-A), five cycles at 200, 500, 800, and 1,000 bars were conducted first, and then, 30 homogenization cycles at 1,200 bars were carried out.

Preparation of SN-38 solution

A total of 100 mg of SN-38 coarse powder was dissolved in a mixture of 4 mL of 1 M NaOH and 2 mL of propylene glycol at 60°C with stirring. Once SN-38 was dissolved, 16 mL of water was added to the solution and the pH was adjusted to 9.6 with 3 M HCl, and then, 0.1 M HCl was added slowly to adjust pH to ~7.4. The solution was filtered through a 0.1 μm microporous membrane to remove the precipitated SN-38. The accurate concentrations was ~4.0 mg/mL, which was determined by high-performance liquid chromatography and mass spectrometry (LC/MS).

Particle size, polydispersity index (PDI), and zeta potential analysis

The mean particle size, PDI, and zeta potential of each SN-38 nanocrystal formulation was determined by dynamic light scattering (Zetasizer Nano-ZS90; Malvern Instruments, Malvern, UK). SN-38 nanocrystals were diluted with deionized water to a suitable scattering intensity before being measured. Then, the samples were analyzed three times with 12 runs in each measurement.

Morphology study

The morphology of SN-38 nanocrystals was observed via a transmission electron microscopy (TEM) instrument (Hitachi 7650; Hitachi Ltd., Tokyo, Japan). One drop of SN-38 nanocrystals was deposited on the surface of copper grids, and then, the samples were air-dried and examined by TEM.

Crystalline state

X-ray powder diffraction (XRPD) analysis was used to evaluate whether the initial crystalline state of powders was maintained before and after particle size reduction. The samples including SN-38 coarse powder, blank excipients, physical mixture of SN-38 and excipients, and two kinds of nanocrystals were analyzed. XRPD diffractograms of all samples were obtained by a D/MAX RB X-ray diffractometer (Rigaku, Tokyo, Japan). XRPD was recorded by Cu Kα radiation source with a wavelength of 1.5405 Å at 40 kV and 100 mA. The range (2θ) of scans was from 5 to 60° at a speed of 2°/min.

LC/MS analysis

The LC/MS method was developed for the determination of SN-38 in all experiments, including the dissolution study, pharmacokinetic experiments, and tissue distribution study. The LC/MS system comprised an Agilent 1200 separation module and an Agilent 6460 triple quadruple mass spectrometer with an atmospheric pressure electro-spray ionization source (Agilent Technologies, Santa Clara, CA, USA). The chromatographic separation was performed on a Poroshell 120 SB-C18 column (2.1×50 mm ×2.7 μm; Agilent Technologies) and maintained at a column temperature of 30°C. The mobile phase consisted of acetonitrile–0.1% formic acid in distilled water (5:95). An aliquot of 5 μL of the final solution was injected into the LC/MS system for analysis, and the flow rate was 0.4 mL/min. The MS condition was as follows: the ion spray voltage at 4,000 V, the nebulizer gas pressure at 45 psi, and nitrogen as drying gas (350°C, 12 L/min). Multiple-reaction monitoring (MRM) operated in positive ion mode was used to determine the analytes, and the quantitative transition m/z values were 393.1/349.2 for SN-38 (collision energy of 24 eV, fragmentation voltage of 147 V) and 349.1/305.3 for CPT (collision energy of 24 eV, fragmentation voltage of 147 V), which was regarded as the internal standard (IS). Scan time was set at 200 ms. Also, the ultraviolet detector was used at 267 nm for measuring the SN-38 concentration of SN-38 nanocrystals and solution before experiments.

Dissolution and stability experiments

The dissolution behavior of SN-38 nanocrystals was evaluated by dialysis. Four groups, including physical mixtures SN-38/NCs-A, SN-38/NCs-B, and SN-38 solution, were diluted by phosphate-buffered saline (PBS; pH 7.4) to 20 μg/mL. A total of 2 mL of each sample was put in a dialysis bag (14,000 Da molecular weight cutoff; Fisherbrand, Pittsburgh, PA, USA), which was then immersed in 200 mL of PBS. The system was shaken at a speed of 150 rpm at 37°C. At predetermined intervals, 0.2 mL of PBS solution with SN-38 outside the dialysis bag was withdrawn for the quantitative analysis of SN-38 concentration.

Meanwhile, stabilities of SN-38 in PBS were evaluated. SN-38/NCs-A, SN-38/NCs-B, and SN-38 solution were put

in 20 mL of PBS (pH 7.4) at the concentration of 20 μg/mL. After 12 h incubation at 37°C, the samples were taken and SN-38 contents were rapidly measured by LC/MS.

Cellular uptake studies

The intracellular SN-38 accumulation was investigated under confocal laser scanning microscopy (UltraVIEW Vox; Perkin-Elmer Inc., Waltham, MA, USA). Briefly, HT1080 cells were seeded into a Petri dish at a density of 18×10^4 cells/well and cultured in a humidified atmosphere containing 5% CO_2 at 37°C for 12 h. Then, the medium was replaced with 1 mL of SN-38/NCs-A, SN-38/NCs-B, or SN-38 solution at the concentration of 20 μg/mL, and the cells were incubated for another 12 h at 37°C. The medium was then removed, and cells were washed with cold PBS (pH 7.4) twice. A total of 2 mL of DID dye diluted with MEM was added, and the cells were maintained at 37°C for 30 min to stain the cell membrane. Then, the cells were washed with cold PBS two times, followed by fixation using 4% paraformaldehyde at 4°C overnight. Besides, nuclei were stained by PI using the same cell lines. At first, following the culture of HT1080 cells for 12 h on a Petri dish, the cells were washed with cold PBS twice, and then fixed using 4% paraformaldehyde at 4°C overnight. Then, cold PBS was added to wash the cells twice, followed by nuclear staining using PI dye diluted with minimum essential medium (MEM) at 37°C for 8 min. The fluorescence images of the cells were observed via CLSM (Waltham, MA, USA) with an emission wavelength of 650 nm for DID, 630 nm for PI, and 550 nm for SN-38.

In vitro cytotoxicity studies

The cytotoxicity of SN-38 nanocrystals and solution on human breast cancer cells MCF-7, fibrosarcoma cells HT1080, and hepatoma cells HepG2 was evaluated by MTT assay. MCF-7 cells were cultured in Roswell Park Memorial Institute (RPMI) 1640 medium supplemented with 10% (v/v) fetal bovine serum (FBS) and 1% (w/v) penicillin–streptomycin in a humidified atmosphere containing 5% CO_2 at 37°C. MEM supplemented with 10% (v/v) FBS and 1% (w/v) penicillin–streptomycin for HT1080 cells and Dulbecco's Modified Eagle's Medium (DMEM) supplemented with 10% (v/v) FBS and 1% (w/v) penicillin–streptomycin for HepG2 cells were used, and the two kinds of cells were also cultured in a humidified atmosphere containing 5% CO_2 at 37°C. The cells were seeded in a 96-well plate at a density of 2×10^4/well for MCF-7, 1×10^4/well for HT1080, and 0.8×10^4/well for HepG2 and grown overnight. Meanwhile, the blank wells without cells, as background group, and the wells with cells, as control group, were established. Then, the media were replaced with different concentrations of SN-38/NCs-A, SN-38/NCs-B, or SN-38 solution for 48 h. A total of 20 μL of MTT solution (0.5 mg/mL) was added to each well, and the cells were incubated for another 4 h at 37°C. Next, the MTT-containing medium was removed, and 200 μL of DMSO was added, and the mixture was shaken at room temperature for 10 min to dissolve the formazan crystals produced by living cells. Finally, a microplate reader (Tecan, Grodig, Austria) was used to measure the optical densities of each well at a wavelength of 492 nm.

Pharmacokinetic evaluation

Nine male Sprague Dawley rats were randomly and equally divided into three groups. Three formulations, including SN-38/NCs-A, SN-38/NCs-B, and SN-38 solution, were administrated intravenously via tail vein to the rats in the three groups at a dose of 5 mg/kg. Orbital blood samples were collected using heparinized tubes at predetermined times and centrifuged at the speed of 4,000 rpm for 10 min immediately. A total of 100 μL of plasma was separated from the supernatant by adding 200 μL of methanol to extract SN-38. Then, 100 μL of camptothecin acetonitrile solution was added at the concentration of 50 ng/mL as IS and vortex-mixed for 1 min. After centrifuging at 14,000 rpm for 10 min, the supernatant was transferred to another tube and evaporated using a rotary evaporator (Labconco Corp, Kansas City, MO, USA) at 40°C for 5 h. The residue was dissolved in 100 μL of acetonitrile–water (80:20) with vortex-mixing for 3 min and centrifuged at 14,000 rpm for 10 min. Finally, 5 μL of supernatant was injected for LC/MS analysis to determine the SN-38 concentration in plasma.

In vivo antitumor efficacy

The antitumor effect was investigated on the female Nu/nu nude mice. Briefly, 0.1 mL of MCF-7 cells (1×10^7/mL) was inoculated subcutaneously in the right armpit of each mouse. When the tumor volume reached ~200 mm^3 at day 8 after the inoculation, the MCF-7-bearing mice were randomly divided into the following four groups (n=6/group): saline, SN-38/NCs-A, SN-38/NCs-B, and SN-38 solution. At days 9, 11, 13, and 15 after the inoculation, the three treatment groups were injected intravenously via the tail vein at the dose of 8 mg/kg, while the control group was administrated saline as negative control. To calculate the tumor volume, the width and length of tumor of each mouse were measured every 2 days with a caliper. Tumor volume was estimated as $[(\text{length})\times(\text{width})^2/2]$.[27] The body weight of each mouse was also weighed every 2 days as an index of systemic toxicity.[28] At day 22, the mice were sacrificed and tumors were excised

and weighed. The survival rate and tumor inhibition rate (IR) were calculated. IR was calculated by $[(W_{control} - W_{treated})/W_{control}]$, here $W_{control}$ was the tumor weight of mice treated with saline and $W_{treated}$ was the tumor weight of mice treated with SN-38 nanocrystals or solution.[28] Besides, HE reagent was used to dye the tumor paraffin sections of the four groups to observe the pathological change.

To investigate the difference of biodistribution of the SN-38/NCs-A, SN-38/NCs-B, and solution, the MCF-7 tumor-xenografted mice were also used. When the tumor volume reached ~300 mm^3, the three formulations were intravenously injected into the mice via tail veins at a dose of 8 mg/kg, respectively. At 1 and 24 h after injection, blood was collected using heparinized tubes and centrifuged immediately to obtain plasma, and the animals were then euthanized to separate organs and tumor samples. All organs and tumors were washed with saline, weighed, and homogenized. Then, the plasma and tissue homogenates were prepared and analyzed using the same method in the "Pharmacokinetic evaluation" section.

Statistical analysis

Data are expressed as mean ± standard deviation (SD) of replicate analyses. A Student's *t*-test was performed to evaluate the results. Differences with *P*-values <0.05 were considered statistically significant.

Results and discussion

Particle size and morphological analysis

Two SN-38 nanocrystal suspensions with different particle sizes were prepared by HPH using different pressures. Figure 1 shows the morphology and particle size distribution of SN-38/NCs-A and SN-38/NCs-B. Under TEM, SN-38/NCs-A and SN-38/NCs-B were cone-shaped. The mean sizes of SN-38/NCs-A and SN-38/NCs-B were 229.5±1.99 nm (Figure 1C) and 799.2±14.44 nm (Figure 1D), respectively. The two SN-38 nanocrystal suspensions were both in the nano-size range with a narrow size distribution. They are suitable for intravenous injection.[29] The PDI values were 0.141±0.015 for SN-38/NCs-A and 0.202±0.067 for SN-38/NCs-B. PDI values <0.3 indicate a narrow size distribution.[30,31]

Zeta potential reflects the electric charge at the surface of particles. It has a significant influence on the physical stability of nanocrystal suspensions.[25] Zeta potential of SN-38/NCs-A and SN-38/NCs-B were −27.1±0.36 mV and −27.6±0.21 mV respectively. Generally, zeta potential of a stable system should be at least 20 mV by using nonionic surfactants for steric hindrance and 30 mV by using ionic surfactants for electric repulsion.[32] In our study, the two SN-38 nanocrystals used Poloxamer 188 and soybean lecithin as stabilizers. The electric and steric effects protected them simultaneously. The zeta potentials of SN-38/NCs-A and SN-38/NCs-B

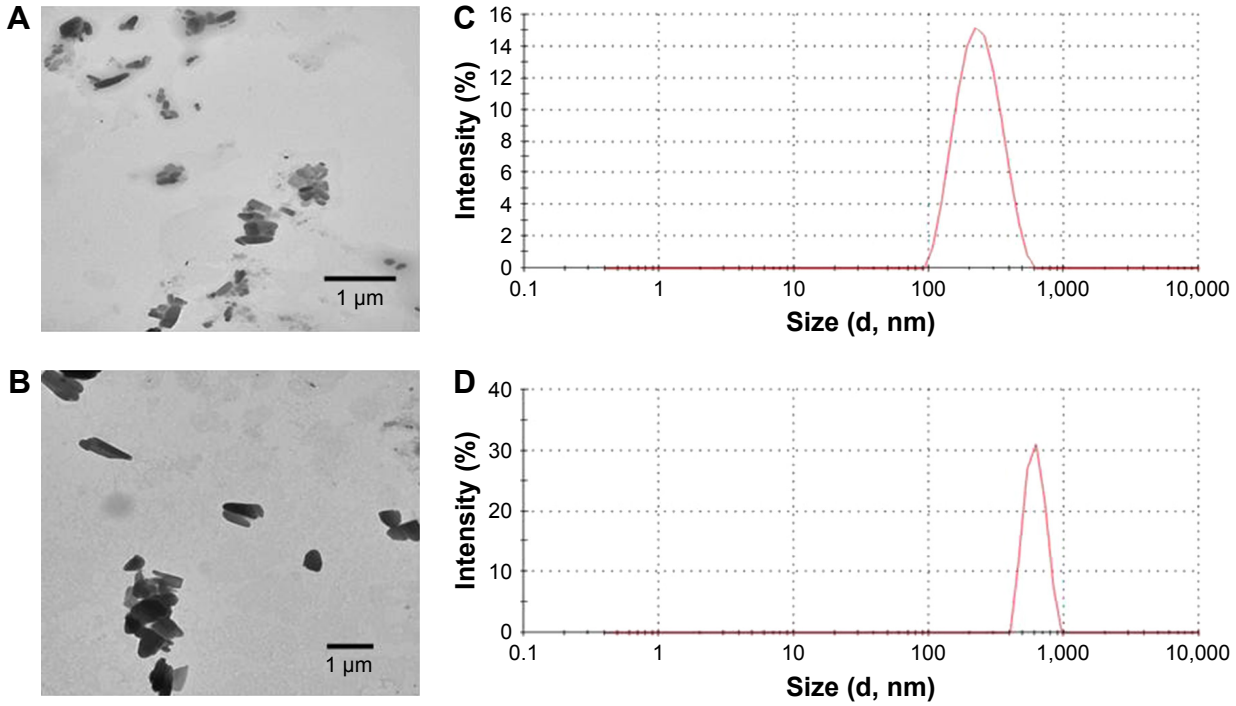

Figure 1 The morphology and particle size distribution of SN-38 nanocrystals.
Notes: (**A**) TEM image of SN-38/NCs-A, (**B**) TEM image of SN-38/NCs-B, (**C**) size distribution of SN-38/NCs-A, and (**D**) size distribution of SN-38/NCs-B.
Abbreviations: SN-38, 7-ethyl-10-hydroxycamptothecin; SN-38/NCs-A, SN-38 nanocrystals A; SN-38/NCs-B, SN-38 nanocrystals B; TEM, transmission electron microscopy.

were ~–27 mV. This benefits the physical stability of the nanocrystal suspensions.

Crystalline state analysis

A crystalline state study was conducted after the HPH process. During HPH, a high energy input caused by the high power density at the piston-gap homogenizer may change the crystalline state.[33,34] The chemical hardness and physical hardness of the active ingredient and the applied power density were the main factors determining the extent of such changes.[35,36] Moreover, the crystalline state is a factor affecting the dissolution rate and physical stability of the nanocrystal suspensions.[37] Thus, before and after the nanosizing process, XRPD study was carried out to evaluate if the initial crystalline state was preserved. The XRPD diagrams of SN-38 coarse powder, blank excipients, physical mixtures, SN-38/NCs-A, and SN-38/NCs-B are shown in Figure 2. The characteristic peaks of SN-38 coarse powder were observed at the 2θ values of 10.38, 10.95, 13.25, 17.74, and 23.90, which were also found in the diffraction patterns of SN-38/NCs-A, SN-38/NCs-B, and physical mixtures. Blank excipients had different diffraction peaks at 19.09 and 23.29, which were also maintained in the profiles of SN-38/NCs-A, SN-38/NCs-B, and physical mixtures simultaneously. These results demonstrated that the nanosizing process via HPH had no influence on the crystalline state of SN-38/NCs-A and SN-38/NCs-B. It also suggested that the enhancement of dissolution velocity of SN-38 might result from the reduction of particle size and the effect of surfactants rather than the changes in crystalline state.

Dissolution experiments

The dissolution release profiles for SN-38/NCs-A, SN-38/NCs-B, physical mixtures, and SN-38 solution were evaluated in PBS (pH 7.4). In order to examine the influence of Poloxamer 188 and soybean lecithin as surfactants on the dissolution rate of SN-38 nanocrystals, the dissolution behavior of physical mixtures was also tested because surfactants have the effects of solubilization, wetting, and emulsification.[37] Figure 3 shows that the dissolution velocity of both SN-38/NCs-A and SN-38/NCs-B were distinctly superior compared to the physical mixture. Meanwhile, the dissolution rate of SN-38/NCs-A was significantly faster than that of SN-38/NCs-B. Within 18 h, 84% of SN-38/NCs-A and 49% of SN-38/NCs-B were detected outside the dialysis membrane, while the amount of physical mixtures was only 32%. This suggests that the nanocrystals could markedly increase the dissolution velocity of SN-38 regardless of the effect of the surfactants. The improved dissolution rate of SN-38 nanocrystals can be explained by the Noyes–Whitney equation: $dc/dt = D \times A \times (Cs - Ct)/h$.[38] In the equation, dc/dt is the dissolution velocity, D is the diffusion coefficient, A is the surface area, h is the diffusion distance, Cs is the saturation solubility, and Ct is the bulk concentration. The equation shows that the dissolution rate of nanocrystals could be increased as the surface area of particles improved, which resulted from the reduction of particle size. Meanwhile, the reduction of particle size can increase the saturation solubility of nanocrystals, which can be described by the Ostwald–Freundlich equation: $\log(Cs/C_\alpha) = 2\sigma V/2.303RT\rho r$, where Cs is the saturation solubility, C_α is the solubility of the solid consisting of large particles, σ is the interfacial

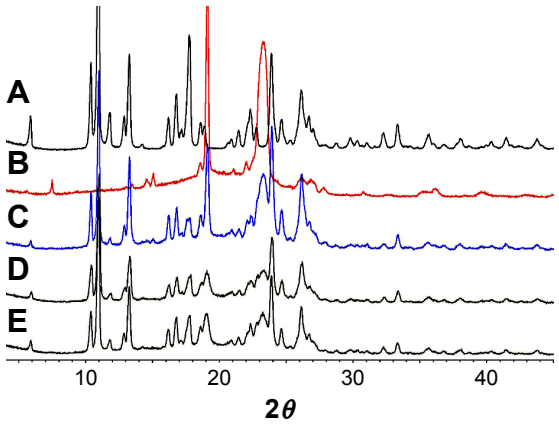

Figure 2 X-ray powder diffraction spectra.
Notes: (**A**) SN-38 coarse powder, (**B**) blank excipients, (**C**) physical mixtures, (**D**) SN-38/NCs-A, and (**E**) SN-38/NCs-B.
Abbreviations: SN-38, 7-ethyl-10-hydroxycamptothecin; SN-38/NCs-A, SN-38 nanocrystals A; SN-38/NCs-B, SN-38 nanocrystals B.

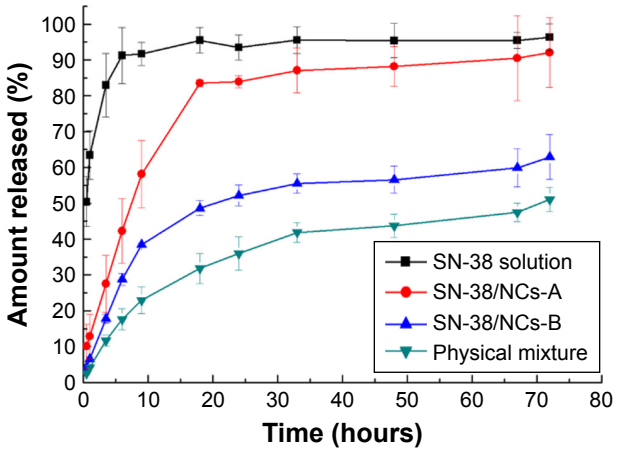

Figure 3 In vitro release profiles of SN-38/NCs-A, SN-38/NCs-B, solution, and physical mixture in pH 7.4 phosphate-buffered saline (n=3).
Abbreviations: SN-38, 7-ethyl-10-hydroxycamptothecin; SN-38/NCs-A, SN-38 nanocrystals A; SN-38/NCs-B, SN-38 nanocrystals B.

tension of substance, V is the molar volume of the particle material, R is the gas constant, T is the absolute temperature, ρ is the density of the solid, and r is the radius of particles.[39] According to the Noyes–Whitney equation, the enhancement of the saturation solubility could also improve the dissolution rate. Therefore, the increased dissolution behaviors of SN-38 nanocrystals were mainly attributed to the enlarged surface area and the increased saturation solubility due to the reduction of particle size rather than the effects of the crystalline form and surfactants.

In contrast, the release rate of SN-38 nanocrystals was significantly slower than that of SN-38 solution. A total of 50% of SN-38 in the solution was released from the dialysis membrane within 0.5 h, while 9 h and 18 h were needed for SN-38/NCs-A and SN-38/NCs-B, respectively. We can infer that it may take a much longer time for a larger amount of SN-38 nanocrystals to dissolve within a smaller volume of medium (eg, in our in vivo study where 1 mg of nanocrystals was injected into a 200 g rat that commonly has 10 mL of plasma for pharmacokinetic evaluation, and 160 μg of nanocrystals was administrated to a 20 g mouse that commonly bears 2 mL of plasma for an antitumor efficacy study). Although the dissolution rate of SN-38 nanocrystals was much slower than that of SN-38 solution, it might be beneficial to prolong the drug delivery circulation and reinforce the enhanced permeability and retention (EPR) effect in vivo. In addition, the stabilities of SN-38/NCs-A and SN-38/NCs-B were significantly higher than SN-38 solution after 12 h incubation at 37°C in pH 7.4 buffer ($P<0.05$). The contents of the active lactone ring were 11.3, 52.1, and 73.6% for SN-38 solution, SN-38/NCs-A, and SN-38/NCs-B, respectively. Therefore, the hydrolysis of the active lactone ring that must occur in solution was restricted in the form of SN-38 solid particles.

Cellular uptake studies

The cellular uptake and intracellular localization of SN-38/NCs-A, SN-38/NCs-B, and SN-38 solution were characterized in HT1080 cells and observed by CLSM. As shown in Figure 4, after 12 h incubation at 37°C, the amount of SN-38 in cells of the SN-38/NCs-A group was much more than that of SN-38/NCs-B and solution groups. Moreover, in the SN-38/NCs-A group, the drug was mainly distributed in the cell nucleus, which was consistent with the anticancer mechanism of SN-38. SN-38 targets the nuclear enzyme TOPI to execute the therapeutic action. In addition, the amount of SN-38 in cells of SN-38/NCs-B and solution groups was not significantly different, and the drug of the two groups was not observed in the cell nucleus after 12 h. Therefore, the ability of cells to uptake SN-38/NCs-A in HT1080 cells was the best among the three formulations. Based on these results, SN-38 nanocrystals may be directly absorbed by the

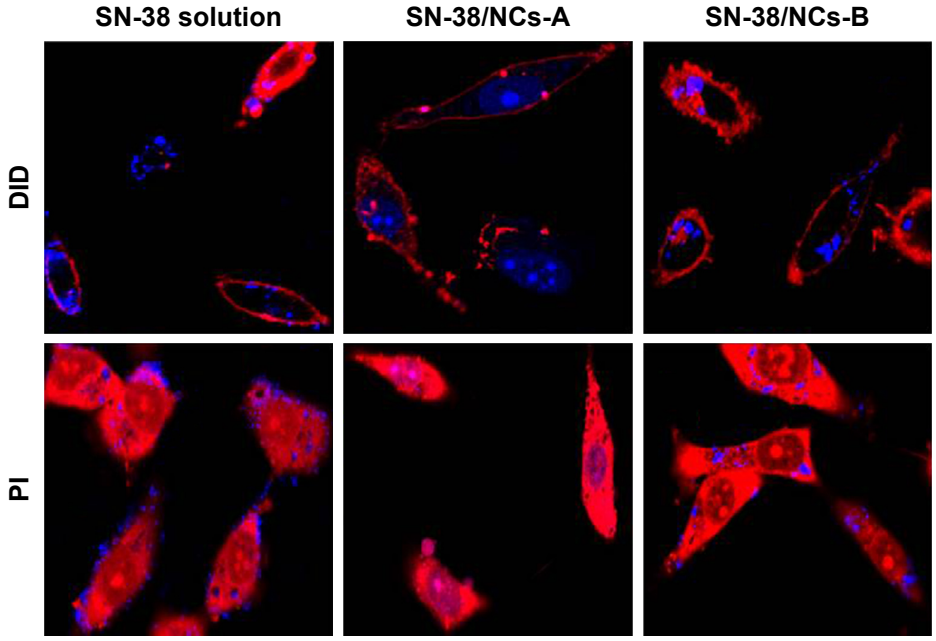

Figure 4 Cellular uptake of the study formulations.
Notes: The CLSM images of HT1080 cellular uptake of SN-38/NCs-A, SN-38/NCs-B, and solution after 12 h of incubation. (In this figure, cell membranes and nuclei were stained by DID and PI, respectively, and both are in red. The blue is the drug). Magnification ×600.
Abbreviations: SN-38, 7-ethyl-10-hydroxycamptothecin; SN-38/NCs-A, SN-38 nanocrystals A; SN-38/NCs-B, SN-38 nanocrystals B; CLSM, confocal laser scanning microscopy; PI, propidium iodide; DID, 1,1′-dioctadecyl-3,3,3′,3′-tetramethylindodicarbocyanine, 4-chlorobenzenesulfonate salt.

cells through multiple endocytosis pathways other than the passive diffusion of free molecules in solution, or dissolved from nanocrystals across the cell membrane.

The internalization pathways of SN-38 nanocrystals depend on their size and may include micropinocytosis, phagocytosis, clathrin-mediated endocytosis, and nonclathrin-mediated endocytosis.[40] Particle size has an important effect on the cellular pathway of entry and subsequent intracellular localization in cells. A report by Rejman et al[40] showed that particles with a diameter of ≤200 nm were internalized via the clathrin-mediated endocytosis, and the caveolae-mediated endocytosis becomes increasingly apparent as size increases (<1 μm). This results in caveolae-mediated endocytosis as the predominant pathway for particles <500 nm.

In our study, the particle sizes of SN-38/NCs-A and SN-38/NCs-B were ~230 and 800 nm, respectively. Therefore, the difference in the cellular internalization pathways of the two SN-38 nanocrystals due to different sizes may be the major factor leading to the significant differences in the cellular uptake of SN-38/NCs-A and SN-38/NCs-B. Overall, the cellular uptake amount of SN-38 was increased after it was made into nanocrystals when compared with SN-38 solution, and nanocrystals with smaller size had significant advantages on cellular uptake.

In vitro cytotoxicity studies

The cytotoxicity of SN-38/NCs-A, SN-38/NCs-B, and SN-38 solution was evaluated in cancerous MCF-7, HT1080, and HepG2 cell lines (Figure 5). As a result, half maximal inhibitory concentrations (IC50) of SN-38/NCs-A, SN-38/NCs-B, and SN-38 solution on MCF-7 cells were 0.031, 0.145, and 0.708 μg/mL, respectively. The difference was statistically significant between any two formulations ($P<0.05$). IC50 values of SN-38/NCs-A, SN-38/NCs-B, and SN-38 solution on HepG2 cells were 0.076, 0.179, and 0.683 μg/mL respectively,

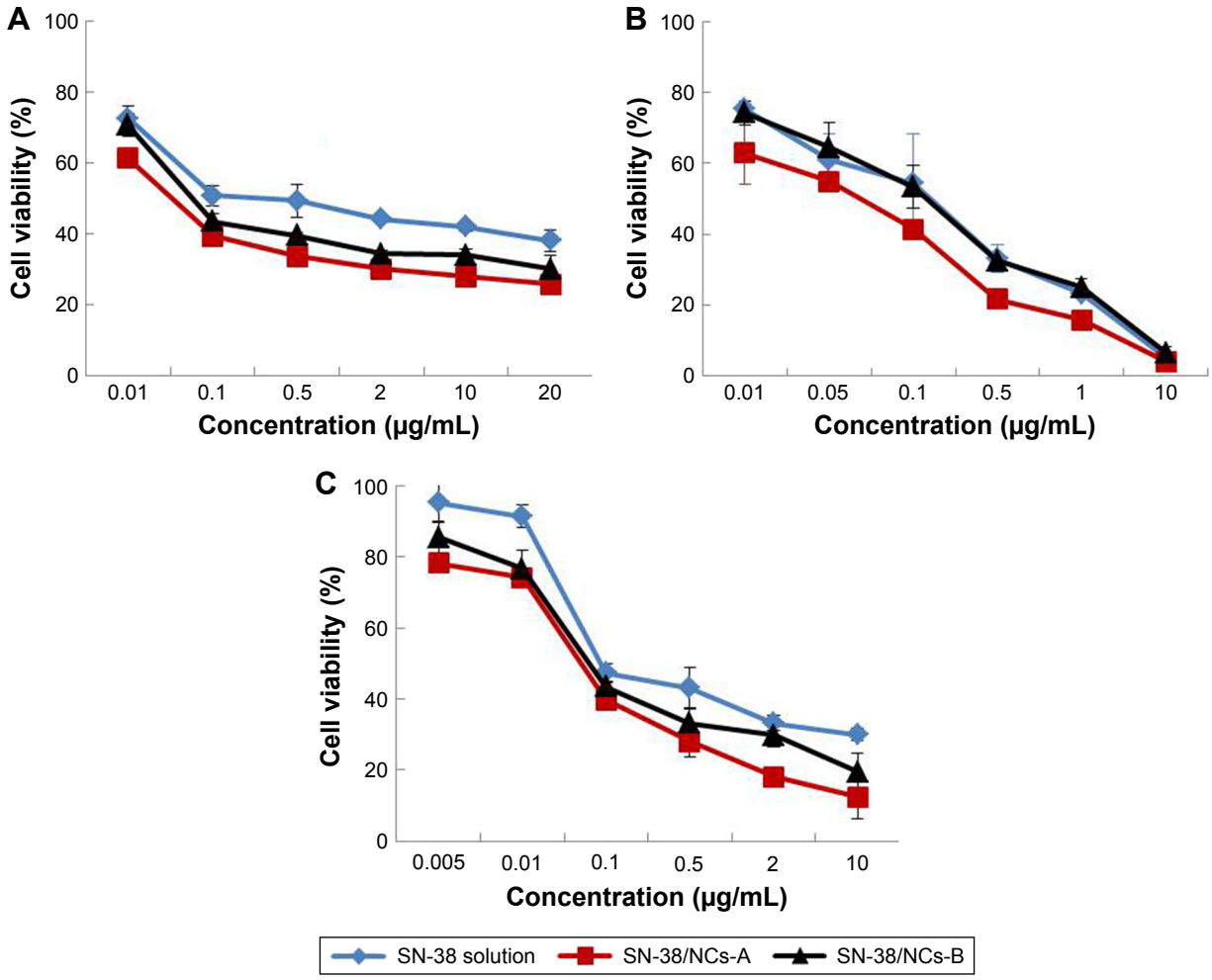

Figure 5 In vitro cytotoxicity of SN-38/NCs-A, SN-38/NCs-B, and solution.
Notes: (**A**) cytotoxicity against MCF-7 cells, (**B**) cytotoxicity against HT1080 cells, and (**C**) cytotoxicity against HepG2 cells (n=3).
Abbreviations: SN-38, 7-ethyl-10-hydroxycamptothecin; SN-38/NCs-A, SN-38 nanocrystals A; SN-38/NCs-B, SN-38 nanocrystals B.

and significant difference was also found between any two groups ($P<0.05$). These results showed that SN-38/NCs-A exhibited significant inhibition on MCF-7 and HepG2 cells when compared with SN-38/NCs-B and SN-38 solution. The cytotoxicity of SN-38/NCs-B for MCF-7 and HepG2 cells were more potent than SN-38 solution. IC50 values of SN-38/NCs-A, SN-38/NCs-B, and SN-38 solution on HT1080 cells were 0.046, 0.111, and 0.104 μg/mL, respectively. SN-38/NCs-A exhibited significantly better antitumor activity against HT1080 cells than SN-38/NCs-B and SN-38 solution ($P<0.05$), but the cytotoxicity of SN-38/NCs-B and SN-38 solution on HT1080 cells was not statistically different ($P>0.05$).

There were some possible explanations for these results. First, the lactone ring of SN-38 was prone to hydrolysis at pH 7.4,[41] and the stability of the lactone ring in SN-38/NCs might be enhanced significantly compared to the solution.[28,42] Second, SN-38 is a P-gp substrate.[43] Part of SN-38 molecules in tumor cells will be transported outside cells by P-gp transporters, while SN-38/NCs-A is not affected by P-gp transporters. Third, when accumulating on the surface of the cancer cells, nanoparticles could be adsorbed by pinocytosis.[44] Eventually, the solubility of drug was improved after nanocrystallization.[39] These reasons might explain the cytotoxic differences among the three formulations.

Pharmacokinetic evaluation

In this experiment, three groups of Sprague Dawley rats were treated with SN-38 solution, SN-38/NCs-A, and SN-38/NCs-B at a dose of 5 mg/kg, respectively. The SN-38 blood concentration–time curves after intravenous administration of different formulations are shown in Figure 6, and the pharmacokinetic parameters are listed in Table 1. Although the peak plasma concentration (C_{max}) for the SN-38 solution group was initially the highest among the three groups, the area under the curve (AUC) of SN-38/NCs-A was subsequently higher than that of SN-38 solution ($P<0.001$). This indicated that nanocrystals with smaller particle size could significantly enhance the drug concentration in blood vs drug solution. The clearance (CL) showed that SN-38 solution was quickly removed from the circulation system, while SN-38/NCs-A represented a markedly delayed blood CL due to the sustained release ($P<0.01$). However, the differences of apparent distribution volume (V) for nanocrystals with smaller particle size and solution were not significant ($P>0.05$). After injection of SN-38/NCs-A, SN-38 was in the form of nanoscale solid particles in plasma, which could prolong the residence time. Moreover, during circulation, some nanoparticles in the SN-38/NCs-A system might be recognized and phagocytized by the reticuloendothelial system (RES). The nanoparticles engulfed by the RES of SN-38/NCs-A might be quickly dissolved in phagocytic cells due to the small particle size. These would be released into blood circulation again to maintain higher and longer blood levels vs SN-38 solution.

For SN-38/NCs-B, however, the results are opposite to the predicted results. The AUC was much lower than that of the SN-38 solution and SN-38/NCs-A. The CL of SN-38/NCs-B was the largest, meaning that the SN-38 in SN-38/NCs-B was removed the fastest. The V and CL of SN-38/NCs-B were significantly different from that of SN-38/NCs-A and solution ($P<0.01$). SN-38/NCs-B with much larger particle sizes might show a slow dissolution behavior in the circulation system as in the in vitro dissolution profiles in Figure 3. Therefore, the slow dissolution

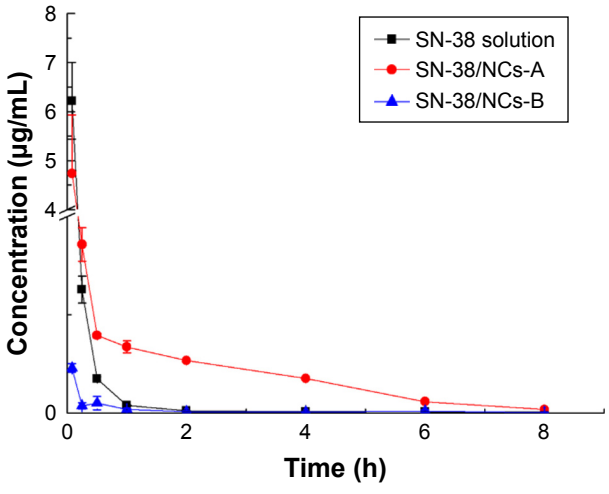

Figure 6 Mean SN-38 concentration–time profiles in plasma after intravenous administration of SN-38/NCs-A, SN-38/NCs-B, and solution to rats at the dose of 5 mg/kg (n=3).
Abbreviations: SN-38, 7-ethyl-10-hydroxycamptothecin; SN-38/NCs-A, SN-38 nanocrystals A; SN-38/NCs-B, SN-38 nanocrystals B.

Table 1 Pharmacokinetic parameters after intravenous administration of SN-38/NCs-A, SN-38/NCs-B, and solution at a dose of 5 mg/kg in Sprague Dawley rats (n=3)

Parameters	Units	SN-38 solution	SN-38/NCs-A	SN-38/NCs-B
$AUC_{(0-t)}$	mg/L h	1.06***	2.06	0.11***
$AUC_{(0-\infty)}$	mg/L h	1.10***	2.09	0.11***
MRT	h	0.92*	1.80	2.29
CL	L/h/kg	4.57***	2.41	45.73**
V	L/kg	4.30	4.33	102.69**
C_{max}	mg/L	6.22*	4.74	0.23***

Note: *$P<0.05$, **$P<0.01$, and ***$P<0.001$, statistical significance compared to SN-38/NCs-A.
Abbreviations: SN-38, 7-ethyl-10-hydroxycamptothecin; SN-38/NCs-A, SN-38 nanocrystals A; SN-38/NCs-B, SN-38 nanocrystals B; CL, clearance; MRT, mean residence time; $AUC_{(0-t)}$, area under the curve from time of administration to time "t"; $AUC_{(0-\infty)}$, area under the curve from time of administration until infinite time elapse; V, apparent distribution volume; C_{max}, peak plasma concentration.

rate in blood circulation might initially cause low plasma concentration in SN-38/NCs-B. The SN-38/NCs-B might be recognized and phagocytized by the RES organs easily and quickly because of the larger particle size after injection. If the solid particles in SN-38/NCs-B system dissolved difficultly in the phagocytic cells, it was hard for the particles to leave the cellular vesicle and enter the blood circulation again. Depending on particle size and composition, the uptake of nanoparticles by organs of RES after intravenous injection might take from a few minutes to many hours.[45] Certainly, further study has to be carried out using the in situ and in vivo models. The related results will be published in other articles.

Overall, these data demonstrated that SN-38/NCs-A with small particle size significantly improved AUC and MRT and decreased CL compared to SN-38 solution. SN-38/NCs-B with large particle size showed the significantly different pharmacokinetic pattern. Therefore, the particle size of SN-38 nanocrystals has a remarkable effect on the pharmacokinetic characters in vivo. It is critical to screen an optimal particle size for nanocrystals for the ideal therapeutic purpose.

In vivo antitumor efficacy

MCF-7-bearing mice were used to evaluate the in vivo anticancer effect of SN-38 nanocrystals and solution. The SN-38/NCs-A, SN-38/NCs-B, and SN-38 solution were administered to each mouse at a dose of 8 mg/kg via tail vein on days 9, 11, 13, and 15 when the tumor volume reached 200 mm^3. The control group was injected with saline. The tumor volume and body weight were measured every 2 days. The tumor growth curves of all groups are shown in Figure 7A and the body weight curve of mice was shown in Figure 7B. The results show that all treatment groups yielded significant tumor repression vs the control group ($P<0.001$ for SN-38/

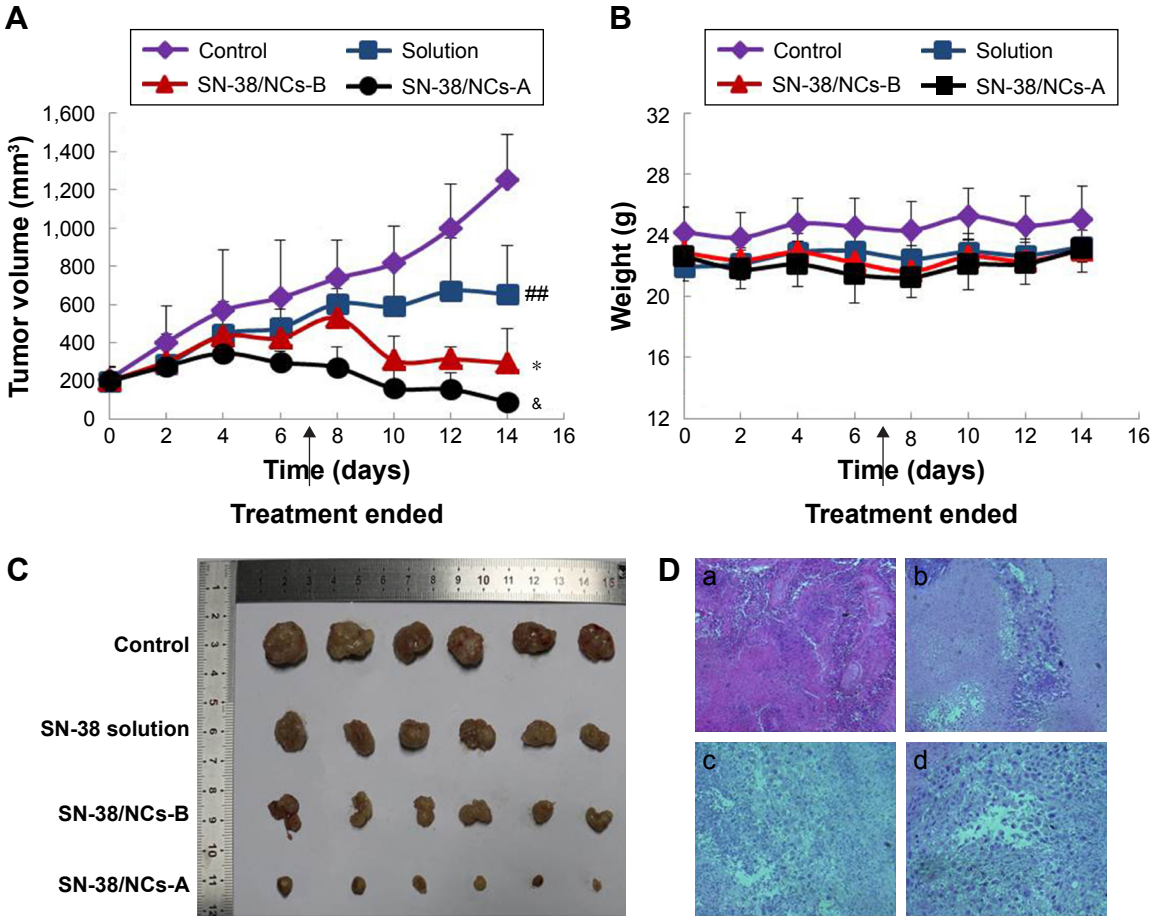

Figure 7 Antitumor effect tested in MCF-7-bearing mice (n=6).

Notes: SN-38/NCs-A, SN-38/NCs-B, or SN-38 solution was administrated to mice via tail vein at the dosage of 8 mg/kg, and saline was used as control. (**A**) The profile change of tumor volume, $^{\#\#}P<0.01$ vs control; $^{*}P<0.05$ vs solution; $^{\&}P<0.05$ vs SN-38/NCs-B. (**B**) The body weight curve of mice. The arrows in parts **A** and **B** shows the day when treatment ended. (**C**) Photo of tumors in each group upon animal termination. (**D**) HE staining of tumor tissue sections. Tumor paraffin sections dyed with HE reagent were well prepared for observation of the pathological change separately under the microscope (×100). The mice were administered (a) saline, (b) SN-38 solution, (c) SN-38/NCs-B, and (d) SN-38/NCs-A.

Abbreviations: HE, hematoxylin–eosin; SN-38, 7-ethyl-10-hydroxycamptothecin; SN-38/NCs-A, SN-38 nanocrystals A; SN-38/NCs-B, SN-38 nanocrystals B.

NCs-A, $P<0.001$ for SN-38/NCs-B, and $P<0.01$ for SN-38 solution). Among the three formulations, SN-38/NCs-A showed the best inhibition effect and the statistical differences were significant ($P<0.001$ vs solution and $P<0.05$ vs SN-38/NCs-B). SN-38/NCs-B was more effective in inhibiting the tumor growth compared to SN-38 solution ($P<0.05$).

At the end of the experiments, all tumors were excised and weighed to calculate the tumor IR. The average tumor weight of the group administered with saline, SN-38 solution, SN-38/NCs-B, or SN-38/NCs-A was 1.01, 0.49, 0.29, or 0.06 g, respectively. The IR of SN-38 solution, SN-38/NCs-B, or SN-38/NCs-A groups was 51.79, 71.63, or 94.39%, respectively, relative to the control group, and the statistical difference between any two groups was significant ($P<0.05$ for SN-38/NCs-B vs solution and $P<0.01$ for SN-38/NCs-A vs SN-38/NCs-B). Figure 7C shows photos of the tumors. The dissected tumors in the mice treated with SN-38/NCs-A were the smallest. The inhibitory effect of SN-38/NCs-B was weaker than that of SN-38/NCs-A but significantly more potent than salt solution. Therefore, all data revealed that the nanocrystal formulation displayed more dramatic antitumor efficacy when compared with solution. SN-38/NCs-A with smaller particle size exerted a better therapeutic effect than SN-38/NCs-B with larger particle size.

After intravenous injection, the molecules of SN-38 solution were directly released into the blood, where the lactone ring was easily hydrolyzed to the open carboxylate form, which has no therapeutic effect.[41] However, the drug molecules in SN-38 nanocrystals were slowly released after injection and the solid particles might restrict the hydrolysis of the active lactone ring, which meant that there was more active drug to kill the tumor cells. Moreover, the circulation of SN-38 in the blood was prolonged by the formulation of nanocrystals, which improved the bioavailability of SN-38 and was conducive to inhibit the tumor growth. Besides, as the drug particles dissolved, the size of the nanocrystals became smaller. These smaller particles were prone to accumulate in the tumor tissues via the EPR effect. Finally, the drug could be taken up not only as free molecules by diffusion but also as nanoparticles by active transport. This considerably increases the antitumor efficacy.

This good result was also confirmed by the HE staining assay. Tumor tissue sections stained with HE were prepared to further investigate the inhibition effect of SN-38 nanocrystals on human xenograft tumors. As shown in Figure 7D, there were rich blood vessels in the tumor tissue of the control group injected with saline; few apoptotic cells were found. However, in the tumor issues administered with solution and nanocrystals, there were visible apoptotic cells. Apparently, mostly cells with enlarged sizes and excessive vacuolization were observed in MCF-7 tumor tissue sections after the injection of SN-38/NCs-A – most tumor cells were apoptotic. In addition, the amount of apoptotic cells of SN-38/NCs-B group was less than that of SN-38/NCs-A group but more than that of SN-38 solution group. Thus, the histology result was consistent with the above tumor inhibition data.

In addition, the body weight changes of all nude mice were monitored during the course of the experiment for the safety evaluation of SN-38 nanocrystals. As shown in Figure 7B, no significant change was found in the body weights of mice injected with SN-38/NCs-A, SN-38/NCs-B, and SN-38 solution during the experimental period and there was no obvious difference in body weights between the treatment groups. This result suggested that there were negligible acute or serious side effects caused by nanocrystals at the test dose.

SN-38 biodistribution in tumor-bearing mice

SN-38 concentrations in the tumor and major organs of the heart, liver, spleen, lung, kidney, and brain were investigated after the treatment of SN-38 nanocrystals and solution at a dose of 8 mg/kg. Figure 8A shows that at 1 h postinjection, SN-38 in the formulations, including SN-38/NCs-A, SN-38/NCs-B, and solution, was detected in all the above tissues. The amount of SN-38 accumulated in liver and spleen of the mice treated with SN-38/NCs-A and SN-38/NCs-B was significantly higher than that treated with solution. This was suspected to be due to the solid particles, which would be taken up by phagocytic cells of the mononuclear phagocyte system (MPS).[46,47]

More interestingly, after 1 h, the SN-38 accumulated in the tumors administered SN-38/NCs-A and SN-38/NCs-B was ~47- and 10-fold as much as that treated with solution, respectively. After 24 h (Figure 8B), the amount of SN-38 in the tumors administered solution significantly decreased, and the drug accumulated in the tumors treated with SN-38/NCs-A and SN-38/NCs-B were 130- and 30-fold higher than that treated with solution, respectively. Obviously, the SN-38 concentration in the tumor of SN-38/NCs-A group was significantly higher than that of SN-38/NCs-B group after injection at 1 h, as well as at 24 h. Therefore, nanocrystals easily accumulated in tumor. In addition, the amount of SN-38 in the liver and spleen of the mice treated with SN-38/NCs-B at 24 h after injection was significantly higher than those administered SN-38/NCs-A, while there was no significant difference in the first 1 h. One possible reason was that after being taken up by RES organs, SN-38/

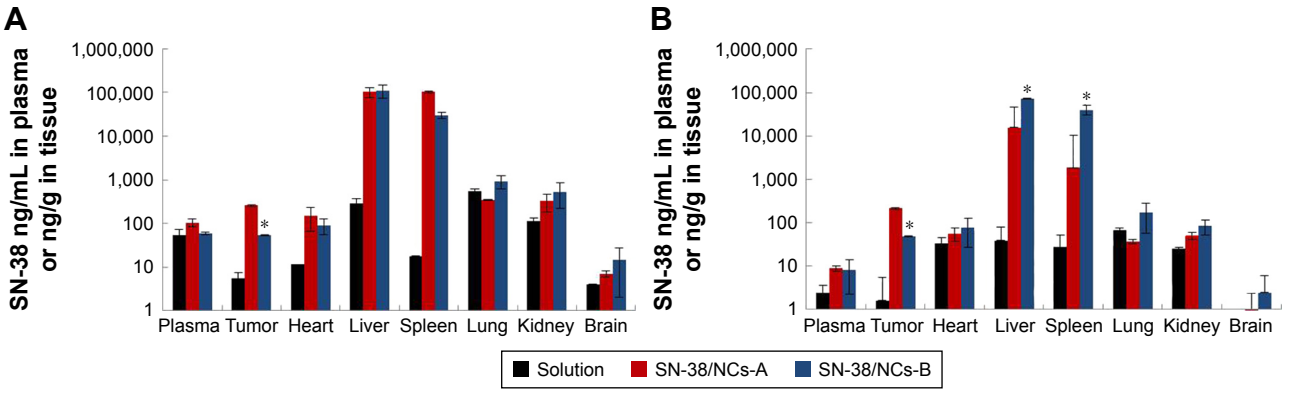

Figure 8 Biodistribution of SN-38 in MCF-7-bearing mice after 1 h (**A**) and 24 h (**B**) treatment with SN-38/NCs-A, SN-38/NCs-B, and solution (n=6).
Note: *$P<0.05$ vs SN-38/NCs-A.
Abbreviations: SN-38, 7-ethyl-10-hydroxycamptothecin; SN-38/NCs-A, SN-38 nanocrystals A; SN-38/NCs-B, SN-38 nanocrystals B.

NCs-A with smaller particle size was prone to dissolve and diffuse into the blood circulation again, but it was hard for SN-38/NCs-B to dissolve and leave the RES organs because of the larger particle size.

The better antitumor efficacy of the two SN-38 nanocrystals was likely attributed to more drug accumulation in the tumor compared to SN-38 solution. The favorable tumor accumulation of SN-38 nanocrystals might result from the EPR effect. As reported in a research study, the vascular pore cutoff of the tumors grown in the subcutaneous microenvironment, depending on the cell line, might range from 200 nm to 1.2 μm and the majority of tumors had a vascular pore cutoff size between 380 and 780 nm.[48] Therefore, the different particle sizes of SN-38/NCs-A and SN-38/NCs-B might be the main factor leading to the significant difference in tumor accumulation between the two nanocrystal formulations. In our study, the mean particle sizes of SN-38/NCs-A and SN-38/NCs-B were ~230 and 800 nm, respectively. SN-38/NCs-A with a smaller mean particle size might be more easily taken up by tumor cells than SN-38/NCs-B in which some particles were >800 nm. Thus, SN-38/NCs-A showed the best tumor accumulation among the three formulations.

Conclusion

This study presents systemic research devised to deal with the drawbacks of SN-38. SN-38 nanocrystals with different particle sizes were successfully developed, and the obtained nanocrystals were cone-shaped. Crystalline state analysis showed that the nanosizing process via HPH had no influence on the crystalline state of SN-38. The dissolution rate increased significantly after dispersion compared to the physical mixture. It was obvious that the particle size of SN-38 nanocrystals had a remarkable influence on dissolution, cellular uptake, pharmacokinetics, tissue distribution, and antitumor efficacy in vitro and in vivo. The in vitro cytotoxicity and cellular uptake studies demonstrated that SN-38/NCs-A with a smaller particle size enhanced the antitumor effect of SN-38 markedly compared to SN-38 solution and SN-38/NCs-B whose particle size was larger. SN-38/NCs-B could induce similar, if not better, anticancer cytotoxic activity compared to the solution. The bioavailability of SN-38 was significantly improved by SN-38/NCs-A by prolonging the blood circulation after intravenous injection, while SN-38/NCs-B showed significantly different pharmacokinetics, such as large MRT, CL, and V, but small AUC. Furthermore, treatment with SN-38/NCs-A had better antitumor effects than treatment with SN-38 solution and SN-38/NCs-B in MCF-7 tumor-bearing mice. Meanwhile, the SN-38/NCs-B inhibited tumor growth significantly vs solution. Therefore, nanocrystals represent a potentially feasible and favorable choice for SN-38 in antitumor research, and it is important to optimize an appropriate particle size for nanocrystals in terms of therapeutic purpose.

Acknowledgments

This work was supported by the National Natural Science Foundation of China under Grant 81573357 and the Beijing Natural Science Foundation under Grant 7162148.

Disclosure

The authors report no conflicts of interest in this work.

References

1. Slatter JG, Su P, Sams JP, Schaaf LJ, Wienkers LC. Bioactivation of the anticancer agent CPT-11 to SN-38 by human hepatic microsomal carboxylesterases and the in vitro assessment of potential drug interactions. *Drug Metab Dispos*. 1997;25(10):1157–1164.

2. Wu MH, Yan B, Humerickhouse R, Dolan ME. Irinotecan activation by human carboxylesterases in colorectal adenocarcinoma cells. *Clin Cancer Res*. 2002;8(8):2696–2700.
3. Zeghari-Squalli N, Raymond E, Cvitkovic E, Goldwasser F. Cellular pharmacology of the combination of the DNA topoisomerase I inhibitor SN-38 and the diaminocyclohexane platinum derivative oxaliplatin. *Clin Cancer Res*. 1999;5(5):1189–1196.
4. Pommier Y. Topoisomerase I inhibitors: camptothecins and beyond. *Nat Rev Cancer*. 2006;6(10):789–802.
5. Zhang JA, Xuan T, Parmar M, et al. Development and characterization of a novel liposome-based formulation of SN-38. *Int J Pharm*. 2004;270(1–2):93–107.
6. Kawato Y, Aonuma M, Hirota Y, Kuga H, Sato K. Intracellular roles of SN-38, a metabolite of the camptothecin derivative CPT-11, in the antitumor effect of CPT-11. *Cancer Res*. 1991;51(16):4187–4191.
7. Zhao H, Rubio B, Sapra P, et al. Novel prodrugs of SN38 using multiarm poly(ethylene glycol) linkers. *Bioconjug Chem*. 2008;19(4):849–859.
8. Thakur R, Sivakumar B, Savva M. Thermodynamic studies and loading of 7-ethyl-10-hydroxycamptothecin into mesoporous silica particles MCM-41 in strongly acidic solutions. *J Phys Chem B*. 2010;114(17):5903–5911.
9. Roger E, Lagarce F, Benoit JP. Development and characterization of a novel lipid nanocapsule formulation of Sn38 for oral administration. *Eur J Pharm Biopharm*. 2011;79(1):181–188.
10. Sapra P, Zhao H, Mehlig M, et al. Novel delivery of SN38 markedly inhibits tumor growth in xenografts, including a camptothecin-11-refractory model. *Clin Cancer Res*. 2008;14(6):1888–1896.
11. Manaspon C, Nittayacharn P, Vejjasilpa K, Fongsuk C, Nasongkla N. SN-38: β-cyclodextrin inclusion complex for in situ solidifying injectable polymer implants. *Conf Proc IEEE Eng Med Biol Soc*. 2011;2011:3241–3244.
12. Matsumura Y. Preclinical and clinical studies of NK012, an SN-38-incorporating polymeric micelles, which is designed based on EPR effect. *Adv Drug Deliv Rev*. 2011;63(3):184–192.
13. Nakajima TE, Yasunaga M, Kano Y, et al. Synergistic antitumor activity of the novel SN-38-incorporating polymeric micelles, NK012, combined with 5-fluorouracil in a mouse model of colorectal cancer, as compared with that of irinotecan plus 5-fluorouracil. *Int J Cancer*. 2008;122(9):2148–2153.
14. Sumitomo M, Koizumi F, Asano T, et al. Novel SN-38-incorporated polymeric micelle, NK012, strongly suppresses renal cancer progression. *Cancer Res*. 2008;68(6):1631–1635.
15. Sadzuka Y, Takabe H, Sonobe T. Liposomalization of SN-38 as active metabolite of CPT-11. *J Control Release*. 2005;108(2–3):453–459.
16. Lei S, Chien PY, Sheikh S, Zhang A, Ali S, Ahmad I. Enhanced therapeutic efficacy of a novel liposome-based formulation of SN-38 against human tumor models in SCID mice. *Anticancer Drugs*. 2004;15(8):773–778.
17. Kurzrock R, Goel S, Wheler J, et al. Safety, pharmacokinetics, and activity of EZN-2208, a novel conjugate of polyethylene glycol and SN38, in patients with advanced malignancies. *Cancer*. 2012;118(24):6144–6151.
18. Vangara KK, Liu JL, Palakurthi S. Hyaluronic acid-decorated PLGA-PEG nanoparticles for targeted delivery of SN-38 to ovarian cancer. *Anticancer Res*. 2013;33(6):2425–2434.
19. Palakurthi S. Challenges in SN38 drug delivery: current success and future directions. *Expert Opin Drug Deliv*. 2015;12(12):1911–1921.
20. Zheng D, Wang Y, Zhang D, et al. In vitro antitumor activity of silybin nanosuspension in PC-3 cells. *Cancer Lett*. 2011;307(2):158–164.
21. Mauludin R, Müller RH, Keck CM. Kinetic solubility and dissolution velocity of rutin nanocrystals. *Eur J Pharm Sci*. 2009;36(4–5):502–510.
22. Merisko-Liversidge E, Liversidge GG, Cooper ER. Nanosizing: a formulation approach for poorly-water-soluble compounds. *Eur J Pharm Sci*. 2003;18(2):113–120.
23. Muller RH, Keck CM. Challenges and solutions for the delivery of biotech drugs – a review of drug nanocrystal technology and lipid nanoparticles. *J Biotechnol*. 2004;113(1–3):151–170.
24. Shi J, Guo F, Zheng A, Zhang X, Sun J. Progress in the study of drug nanocrystals. *Pharmazie*. 2015;70(12):757–764.
25. Liu G, Zhang D, Jiao Y, et al. In vitro and in vivo evaluation of riccardin D nanosuspensions with different particle size. *Colloids Surf B Biointerfaces*. 2013;102:620–626.
26. Leng D, Chen H, Li G, et al. Development and comparison of intramuscularly long-acting paliperidone palmitate nanosuspensions with different particle size. *Int J Pharm*. 2014;472(1–2):380–385.
27. Mamot C, Drummond DC, Noble CO, et al. Epidermal growth factor receptor-targeted immunoliposomes significantly enhance the efficacy of multiple anticancer drugs in vivo. *Cancer Res*. 2005;65(24):11631–11638.
28. Zhang H, Hollis CP, Zhang Q, Li T. Preparation and antitumor study of camptothecin nanocrystals. *Int J Pharm*. 2011;415(1–2):293–300.
29. Möschwitzer J, Achleitner G, Pomper H, Müller RH. Development of an intravenously injectable chemically stable aqueous omeprazole formulation using nanosuspension technology. *Eur J Pharm Biopharm*. 2004;58(3):615–619.
30. Ali HS, York P, Blagden N. Preparation of hydrocortisone nanosuspension through a bottom-up nanoprecipitation technique using microfluidic reactors. *Int J Pharm*. 2009;375(1–2):107–113.
31. Patravale VB, Date AA, Kulkarni RM. Nanosuspensions: a promising drug delivery strategy. *J Pharm Pharmacol*. 2004;56(7):827–840.
32. Jacobs C, Kayser O, Müller RH. Nanosuspensions as a new approach for the formulation for the poorly soluble drug tarazepide. *Int J Pharm*. 2000;196(2):161–164.
33. Möschwitzer J, Müller RH. Spray coated pellets as carrier system for mucoadhesive drug nanocrystals. *Eur J Pharm Biopharm*. 2006;62(3):282–287.
34. Kocbek P, Baumgartner S, Kristl J. Preparation and evaluation of nanosuspensions for enhancing the dissolution of poorly soluble drugs. *Int J Pharm*. 2006;312(1–2):179–186.
35. Teeranachaideekul V, Junyaprasert VB, Souto EB, Müller RH. Development of ascorbyl palmitate nanocrystals applying the nanosuspension technology. *Int J Pharm*. 2008;354(1–2):227–234.
36. Müller RH, Jacobs C, Kayser O. Nanosuspensions as particulate drug formulations in therapy. Rationale for development and what we can expect for the future. *Adv Drug Deliv Rev*. 2001;47(1):3–19.
37. Hao L, Wang X, Zhang D, et al. Studies on the preparation, characterization and pharmacokinetics of Amoitone B nanocrystals. *Int J Pharm*. 2012;433(1–2):157–164.
38. Dressman JB, Amidon GL, Reppas C, Shah VP. Dissolution testing as a prognostic tool for oral drug absorption: immediate release dosage forms. *Pharm Res*. 1998;15(1):11–22.
39. Müller RH, Peters K. Nanosuspensions for the formulation of poorly soluble drugs: I. Preparation by a size-reduction technique. *Int J Pharm*. 1998;160(2):229–237.
40. Rejman J, Oberle V, Zuhorn IS, Hoekstra D. Size-dependent internalization of particles via the pathways of clathrin- and caveolae-mediated endocytosis. *Biochem J*. 2004;377(pt 1):159–169.
41. Bala V, Rao S, Boyd BJ, Prestidge CA. Prodrug and nanomedicine approaches for the delivery of the camptothecin analogue SN38. *J Control Release*. 2013;172(1):48–61.
42. Tang XJ, Han M, Yang B, et al. Nanocarrier improves the bioavailability, stability and antitumor activity of camptothecin. *Int J Pharm*. 2014;477(1–2):536–545.
43. Chu C, Abbara C, Tandia M, et al. Cetuximab increases concentrations of irinotecan and of its active metabolite SN-38 in plasma and tumour of human colorectal carcinoma-bearing mice. *Fundam Clin Pharmacol*. 2014;28(6):652–660.
44. des Rieux A, Fievez V, Garinot M, Schneider YJ, Préat V. Nanoparticles as potential oral delivery systems of proteins and vaccines: a mechanistic approach. *J Control Release*. 2006;116(1):1–27.
45. Manjunath K, Venkateswarlu V. Pharmacokinetics, tissue distribution and bioavailability of clozapine solid lipid nanoparticles after intravenous and intraduodenal administration. *J Control Release*. 2005;107(2):215–228.
46. Rabinow BE. Nanosuspensions in drug delivery. *Nat Rev Drug Discov*. 2004;3(9):785–796.

47. Ganta S, Paxton JW, Baguley BC, Garg S. Formulation and pharmacokinetic evaluation of an asulacrine nanocrystalline suspension for intravenous delivery. *Int J Pharm*. 2009;367(1–2):179–186.
48. Hobbs SK, Monsky WL, Yuan F, et al. Regulation of transport pathways in tumor vessels: role of tumor type and microenvironment. *Proc Natl Acad Sci U S A*. 1998;95(8):4607–4612.